Cell Reports, Volume *14*

Supplemental Information

Control of Smc Coiled Coil Architecture by the ATPase Heads Facilitates Targeting to Chromosomal ParB/*parS* and Release onto Flanking DNA

Anita Minnen, Frank Bürmann, Larissa Wilhelm, Anna Anchimiuk, Marie-Laure Diebold-Durand, and Stephan Gruber

I.) Supplemental Data

Figure S1 Expression, functionality and localization of ATPase mutant Smc proteins. Related to Figure 1.

(A) Colony formation assay using strains BSG1002, 1007, 1045, 1047, 1046, 1008 and 1083. Notably, Smc(EQ) mutant cells form colonies on minimal medium slightly more slowly than wild type or *smc* deletion mutants, suggesting that the mutant protein is mildly toxic when normal Smc function is lacking (Figure S1C, D) (Schwartz and Shapiro, 2011). The slow growth is likely due to a defect in replication origin segregation (Gruber et al., 2014; Schwartz and Shapiro, 2011; Wang et al., 2014), which provides a plausible explanation for the lower number of (replication origin-proximal) Smc foci in Smc(EQ) cells (see Figure S1H). (B) Protein extracts stained by Commassie Brilliant Blue. Immunoblotting of identical protein samples is shown in Figure 1B. (C) Same as in (A) with strains BSG1002, 1007, 1008, 1067, 1068 and 1855. (D) Immunoblotting of extracts from strains BSG1002, 1067, 1855, 1857, 1856, 1068, 1881, 1378, 1413, 1677, 1662, 1799 and 1798 with anti-GFP antiserum (top panel). SDS-PAGE of identical extracts stained by Commassie Brilliant Blue (bottom panel). (E) Immunoblotting against Smc protein using strains BSG1007, 1067, 1002, 1045, 1046, 1008, 2050, 2051. (F) Colony formation assay using strains BSG1002, 1007, 1045, 1046, 1008, 2050 and 2051. (G) ChIP-qPCR using anti-Smc antiserum on strains BSG1002, 1008, 1045, 1046, 2050 and 2051. (H) Quantification of Smc-GFP foci in strains shown in Figure 1C. Number of foci is displayed per unit cell length (µm). Standard deviation is derived from four different fields of view for each genotype. 'n' denotes the total number of individual cells counted.

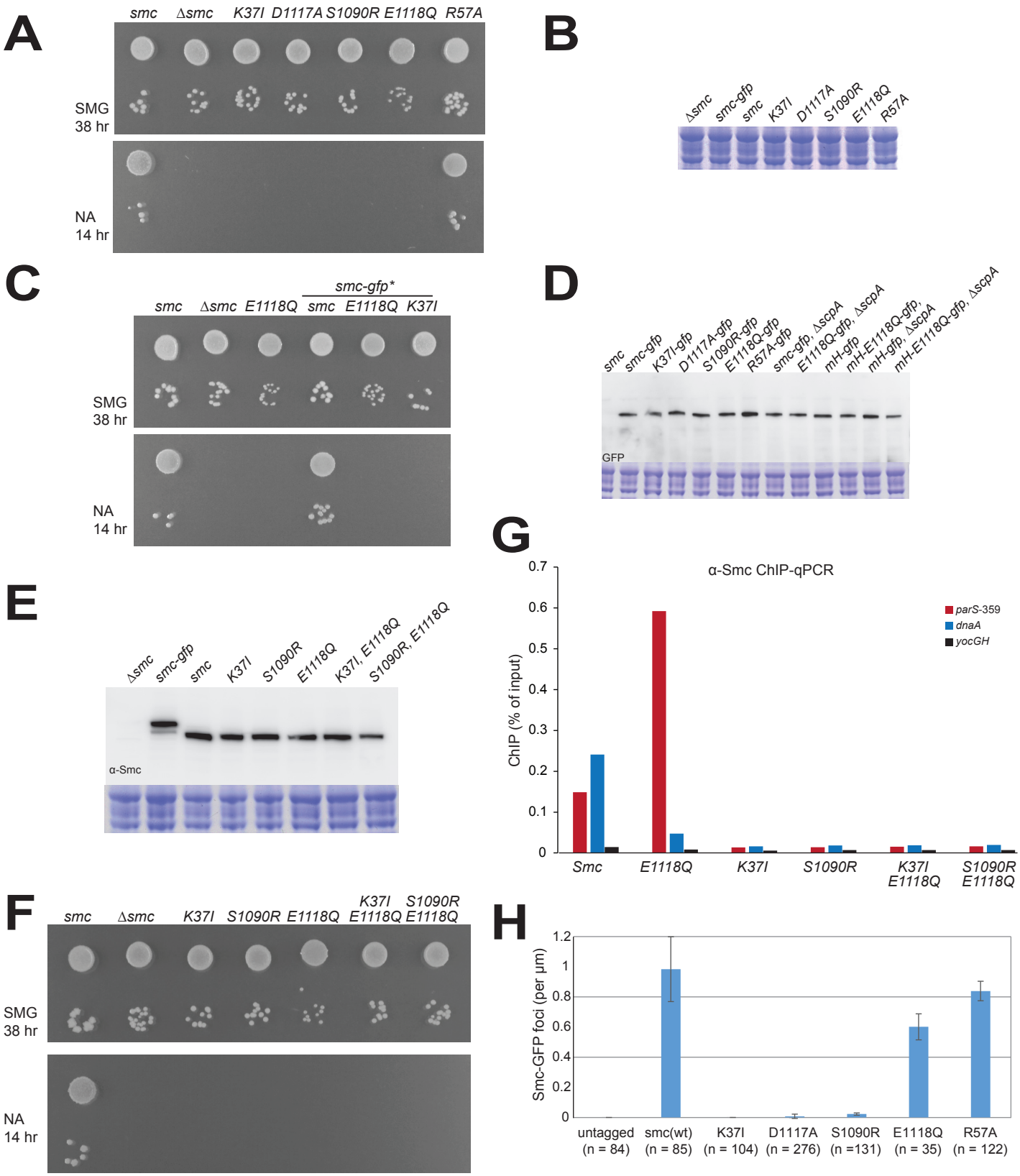
A
smc
Δsmc
K37I
D1117A
S1090R
E1118Q
R57A
SMG
38 hr
NA
14 hr
B
Δsmc
smc-gfp
smc
K37I
D1117A
S1090R
E1118Q
R57A
C
smc-gfp*
smc
Δsmc
E1118Q
smc
E1118Q
K37I
SMG
38 hr
NA
14 hr
D
smc
smc-gfp
K37I-gfp
D1117A-gfp
S1090R-gfp
E1118Q-gfp
R57A-gfp
smc-gfp, ΔscpA
E1118Q-gfp, ΔscpA
mH-gfp
mH-E1118Q-gfp, ΔscpA
mH-gfp, ΔscpA
mH-E1118Q-gfp, ΔscpA
GFP
E
Δsmc
smc-gfp
smc
K37I
S1090R
E1118Q
K37I, E1118Q
S1090R, E1118Q
α-Smc
G
α-Smc ChIP-qPCR
ChIP (% of input)
0.7
0.6
0.5
0.4
0.3
0.2
0.1
0
parS-359
dnaA
yocGH
Smc
E1118Q
K37I
S1090R
K37I E1118Q
S1090R E1118Q
F
smc
Δsmc
K37I
S1090R
E1118Q
K37I E1118Q
S1090R E1118Q
SMG
38 hr
NA
14 hr
H
Smc-GFP foci (per μm)
1.2
1
0.8
0.6
0.4
0.2
0
untagged (n = 84)
smc(wt) (n = 85)
K37I (n = 104)
D1117A (n = 276)
S1090R (n =131)
E1118Q (n = 35)
R57A (n = 122)

Figure S1

Figure S2 Smc and ScpB ChIP-Seq in Smc and Smc(EQ) cells. Related to Figure 2.
(A) ChIP-Seq analysis of BSG1002 and 1008 using anti-Smc antiserum. Number of reads in 1 kb windows at 100bp intervals are shown for input (IN) and ChIP (IP) samples without prior normalization for input material. Normalized data of the same experiment is shown in Figure 2A and 2C. (B) ChIP-Seq analysis of strains BSG1470 and BSG1472 using anti-ScpB antiserum. Data analysis and display as in (A). (C) Whole-genome ChIP-Seq profile for anti-ScpB ChIP (on strain BSG1470), (also shown in Fgiure 7B; same experiment as in Figure S2B). Sequencing reads are put into 5 kb bins and normalized for input DNA. Please note the generally high degree of similarity between anti-Smc (Figure 2C) and anti-ScpB ChIP-Seq profiles with the ScpB profile possibly displaying a steeper gradient from the replicaton origin to the terminus (Kleine Borgmann et al., 2013). (D) Localization of Smc, Smc(S1090R) and Smc(E1118Q) to sites located on the chromosome arm analyzed by ChIP-qPCR using strains BSG1002, BSG1046 and BSG1008. Mean and standard deviation are calculated from three replicate experiments. Boxed insert displays results from the same experiment with “background” correction by subtraction of ChIP obtained with Smc(S1090R).

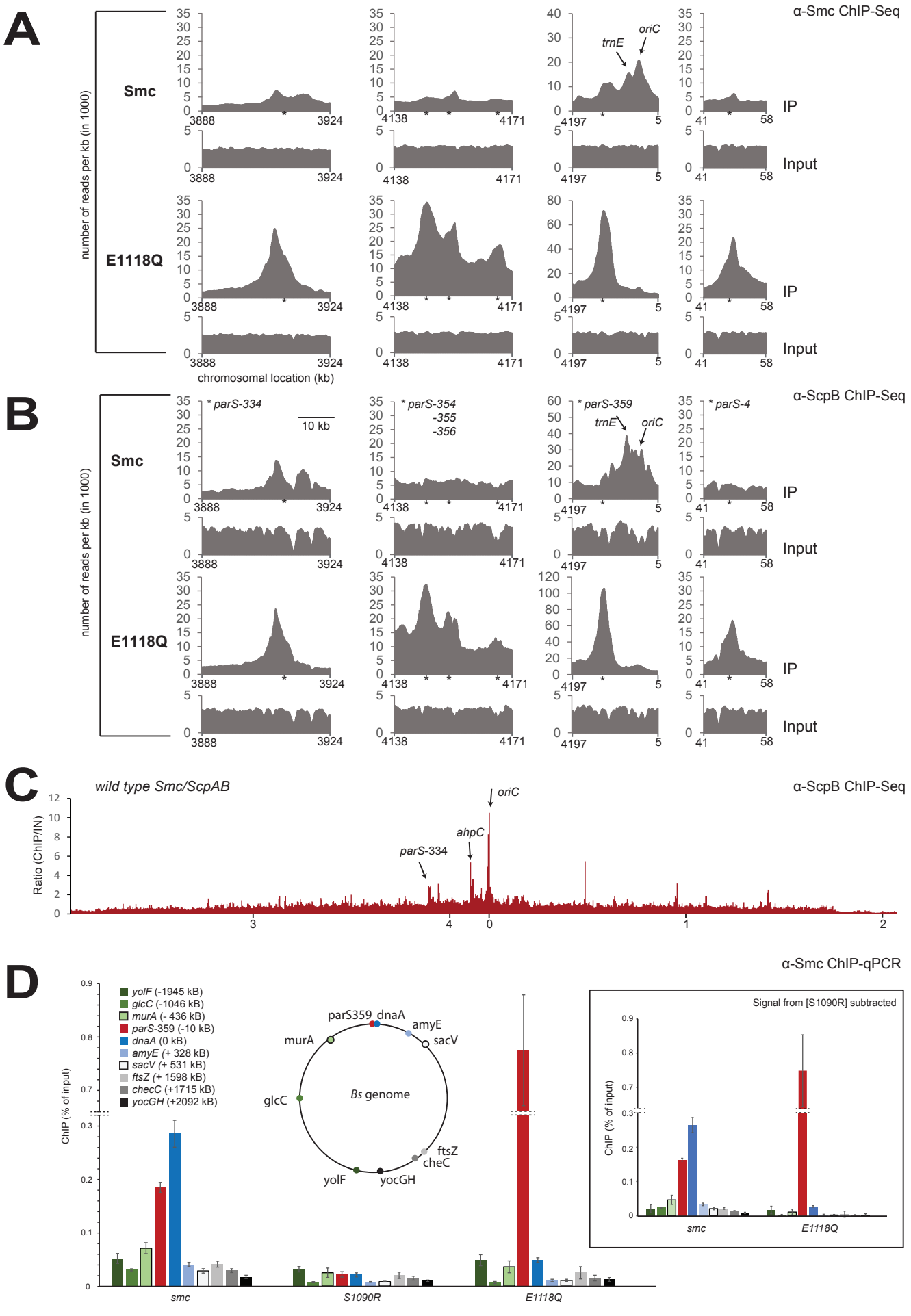
A
α-Smc ChIP-Seq
Smc
E1118Q
IP
Input
number of reads per kb (in 1000)
chromosomal location (kb)
trnE
oriC
B
α-ScpB ChIP-Seq
* parS-334
10 kb
* parS-354
-355
-356
* parS-359
* parS-4
C
wild type Smc/ScpAB
α-ScpB ChIP-Seq
Ratio (ChIP/IN)
parS-334
ahpC
oriC
D
α-Smc ChIP-qPCR
yolF (-1945 kB)
glcC (-1046 kB)
murA (- 436 kB)
parS-359 (-10 kB)
dnaA (0 kB)
amyE (+ 328 kB)
sacV (+ 531 kB)
ftsZ (+ 1598 kB)
checC (+1715 kB)
yocGH (+2092 kB)
ChIP (% of input)
parS359 dnaA
amyE
sacV
murA
glcC
Bs genome
ftsZ
cheC
yolF
yocGH
smc
S1090R
E1118Q
Signal from [S1090R] subtracted

Figure S2

Figure S3 Dimerization at the Smc hinge determines localization of Smc/ScpAB to *parS*. Related to Figure 3.

(A) Immunoblotting of cell extracts from strains BSG1007, 1067, 1002, 1051, 1406, 1052, 1387, 1890, 1893, 1889, 1891 and 1892 using anti-Smc antiserum. (B) Colony formation *Bs* strains BSG1007, 1008, 1889, 1892 and 1891 on minimal medium (SMG). (C) The hinge mutation (GGGG->AAAA) blocks dimerization of headless Smc protein (*Bs*SmcH-CC300). 40 µg of purified proteins was injected onto a gel filtration column and analyzed by multi-angle light scattering (SEC-MALS). Absorbance (at A_{280}) and light scattering is shown for wild-type and hinge mutant *Bs*SmcH-CC300 (curves in red and blue colours, respectively). (D) Analysis of the major peak (in A_{280} absorbance) in SEC-MALS (as in C) of wild-type and hinge-mutant *Bs*SmcH-CC300 indicates the existence of largely dimeric and monomeric protein species, respectively. (E) Immunoblotting of cell extracts from strains BSG1007, 1067, 1002, 1890, 1893, 1892, 1624, 1621 and 1620 using anti-Smc antiserum. (F) Colony formation of strains BSG1007, 1893, 1624, 1621, 1623 and 1620 on minimal medium (SMG). (G) Quantification of Smc-GFP foci in strains shown in Figure 3D. Number of foci is displayed per unit cell length (µm). Standard deviation is derived from four different fields of view for each genotype. 'n' denotes the total number of individual cells counted. (H) ChIP-qPCR analysis of strains BSG1893, 1892, 2144-2147 grown in SMG medium with anti-Smc antiserum.

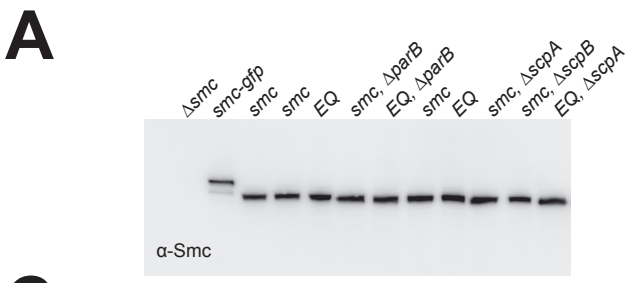

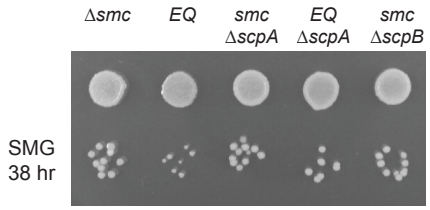

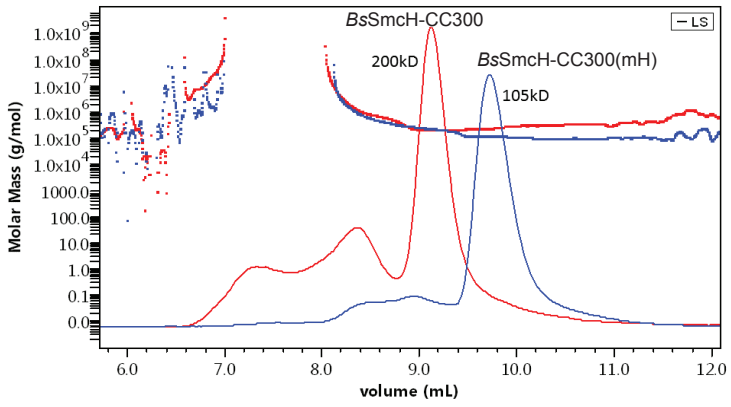

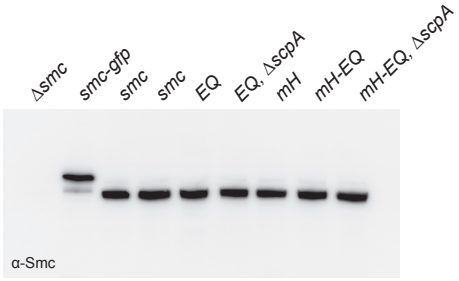

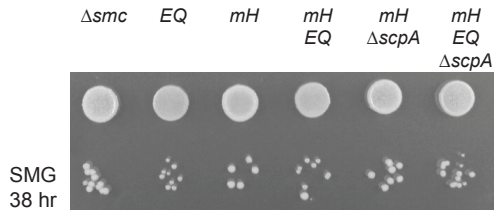

D

	BsSmcH-CC300	BsSmcH-CC300(mH)
Peak analysis (ml)	8.836-9.809	9.404-10.993
Masses		
Injected mass	40µg	40µg
Calculated mass	25.87µg	48.55µg
Mass recovery	64.7%	121.4%
Mass fraction	82.3%	89.1%
Molar mass moments		
Mw	205816.77g/mol	106838.13g/mol
Polydispersity		
Mw/Mn	1.003	1.004
Rms radius moments		
Rz	19.7nm	14.7nm

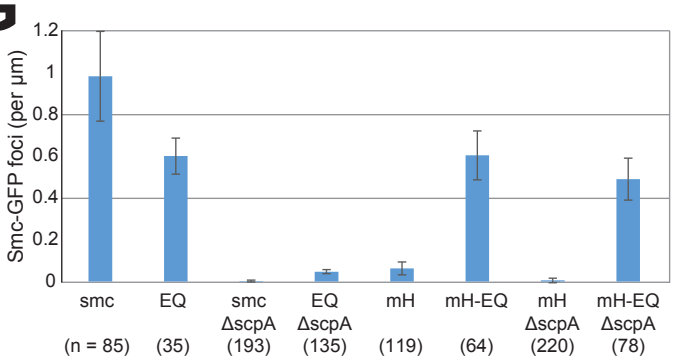

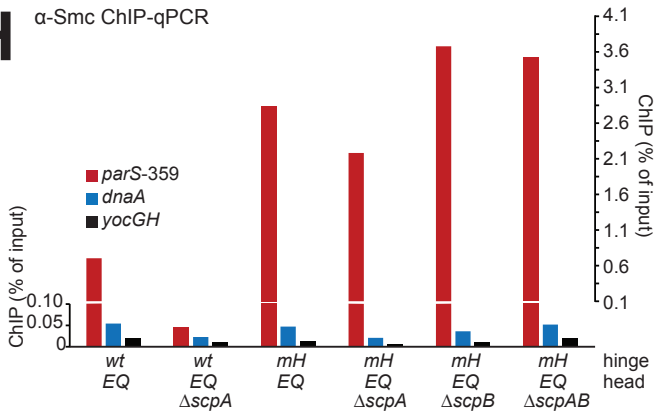

Figure S3

Figure S4 Smc(K1151C) –the reporter for head engagement– is functional. Related to Figure 4.
(A) Colony formation of strains BSG1002, 1007, 1360 and 1457 on minimal medium (SMG) and nutrient rich medium (NA). (B) Cross-linking of Smc(K1151C) in BSG1607, 1488, 1512 and 1513 with BMOE. Mean values and standard deviation from triplicate experiments are shown.

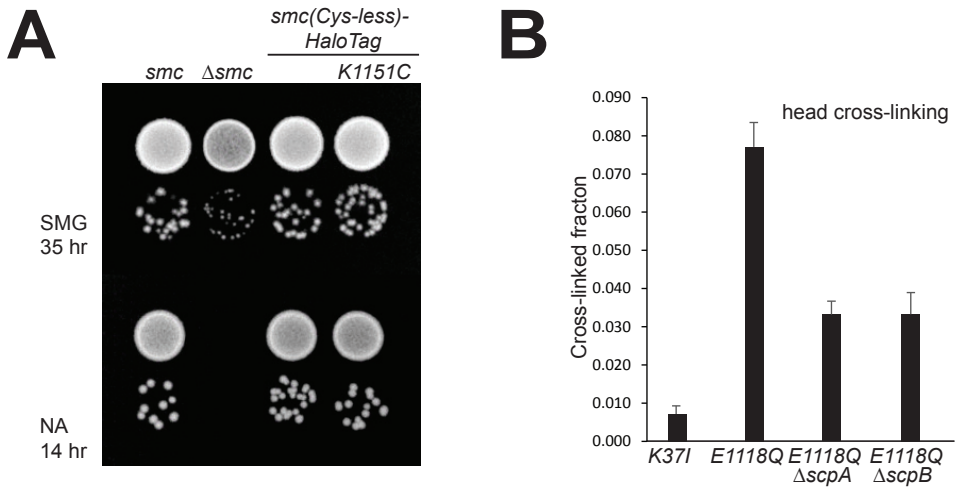
A
smc(Cys-less)-HaloTag
smc
Δsmc
K1151C
SMG 35 hr
NA 14 hr
B
head cross-linking
Cross-linked fracton
0.090
0.080
0.070
0.060
0.050
0.040
0.030
0.020
0.010
0.000
K37I
E1118Q
E1118Q ΔscpA
E1118Q ΔscpB

Figure S4

Figure S5 Expression and functionality of hinge-less Smc protein. Related to Figure 5.
(A) Immunoblotting against the TAP tag on Smc in cell extracts from strains BSG1002, 1016, 1475, 1691, 1896, 1671, 1780, 1672, 1895, 1689 and 1779. Commassie staining of the same extracts is shown in the bottom panel. (B) Colony formation assay using strains BSG1007, 1008, 1626, 1619, 1896 and 1780. (C) Same as in (B) with strains BSG1002, 1007, 1008, 1520, 1689 and 1779. (D) Exemplary image of the SDS-PAGE analysis of disulfide cross-linked *Bs*SmcH-CC300 samples harboring pairs of cysteines as annotated. (E) Quantification of intra- and inter-molecular disulfide formation (after 4 hr incubation) from Commassie stained SDS-PAGE gels for 16 pairs of cysteine mutants. (F) Schematic view of the folding of the Smc coiled coil. Anchor points setting the register of the Smc coiled coils – established by *in vitro* disulfide formation (see D and E)– are given as dashed lines connecting N- and C-terminal helix. Disruptions in the coiled coil register were detected by Marcoil prediction. The length of extra sequences in the C-terminal coiled coil as given by the experimentally determined coiled coil register are indicated at the corresponding positions. Regions relevant for the targeting of mini-Smc to *parS* are highlighted by labels in red colours.

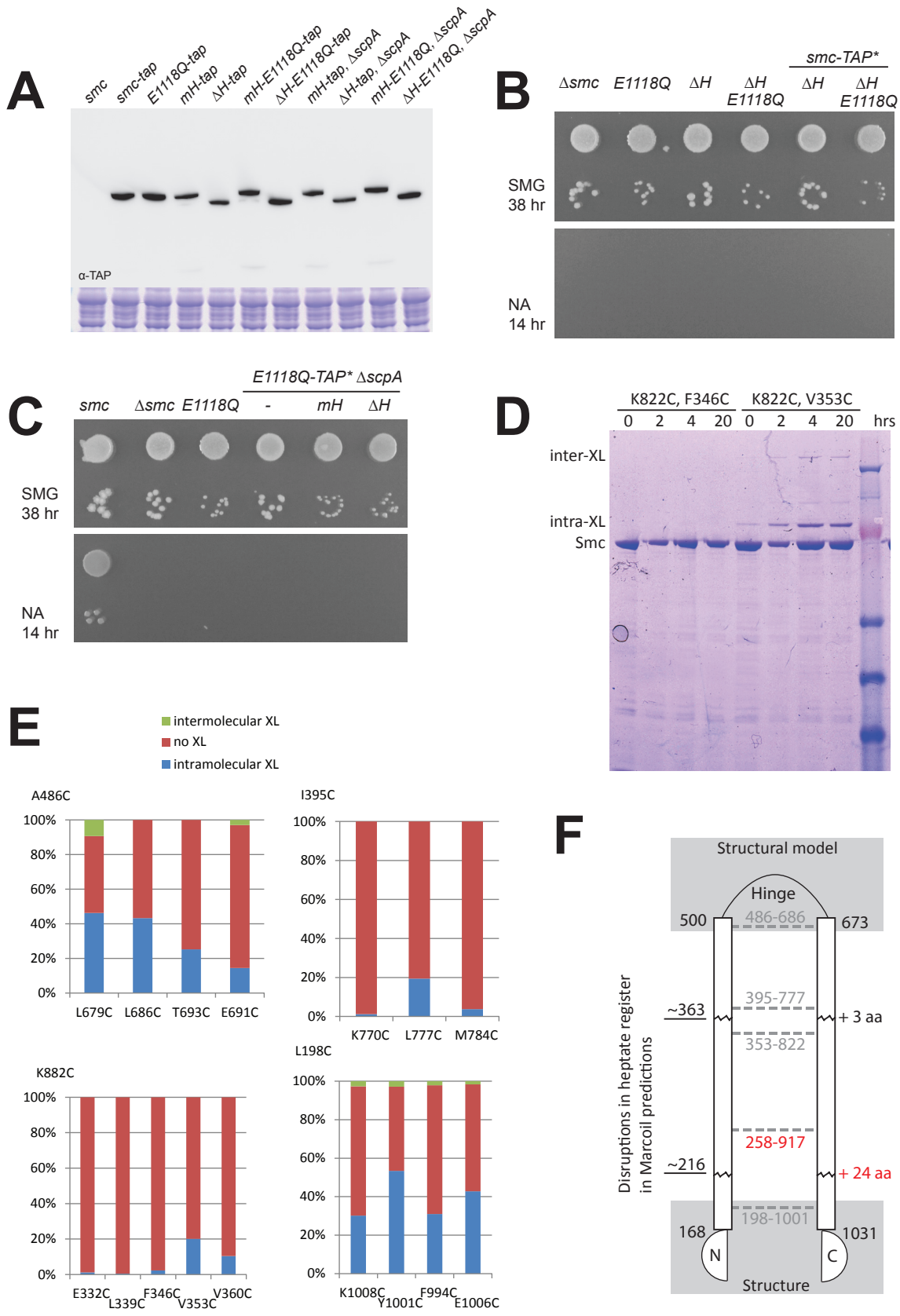
A
smc
smc-tap
E1118Q-tap
mH-tap
ΔH-tap
mH-E1118Q-tap
ΔH-E1118Q-tap
mH-tap, ΔscpA
ΔH-tap, ΔscpA
mH-E1118Q, ΔscpA
ΔH-E1118Q, ΔscpA
α-TAP
B
Δsmc
E1118Q
ΔH
ΔH E1118Q
smc-TAP*
ΔH
ΔH E1118Q
SMG 38 hr
NA 14 hr
C
E1118Q-TAP* ΔscpA
smc
Δsmc
E1118Q
-
mH
ΔH
SMG 38 hr
NA 14 hr
D
K822C, F346C
K822C, V353C
0 2 4 20 0 2 4 20 hrs
inter-XL
intra-XL
Smc
E
intermolecular XL
no XL
intramolecular XL
A486C
100%
80%
60%
40%
20%
0%
L679C L686C T693C E691C
I395C
K770C L777C M784C
K882C
E332C L339C F346C V353C V360C
L198C
K1008C Y1001C F994C E1006C
F
Structural model
Hinge
500
486-686
673
~363
395-777
+ 3 aa
353-822
258-917
~216
+ 24 aa
198-1001
168
1031
N
C
Structure
Disruptions in heptate register in Marcoil predictions

Figure S5

Figure S6 ChIP-Seq of Smc(EQ) to an ectopic *parS* site. Related to Figure 6.
Smc(EQ) is efficiently targeted to *parS-amyE*. ChIP-Seq analysis of BSG1471 (top panel) and BSG1008 (bottom panel) using anti-Smc antiserum. ChIP eluate sequence reads were mapped to 5 kb bins and normalized for input DNA. Please note that Smc(EQ) localization to endogenous parS sites is decreased by the presence of an extra *parS* site, being consistent with a titration effect. The bottom panel is identical to the bottom panel of Figure 2C.

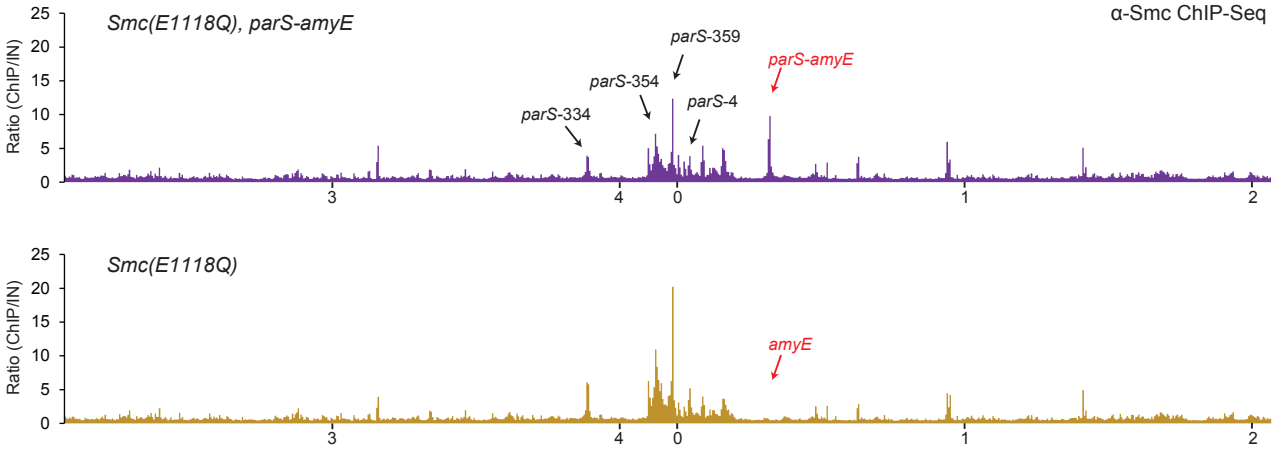
Smc(E1118Q), parS-amyE
α-Smc ChIP-Seq
Ratio (ChIP/IN)
parS-359
parS-amyE
parS-354
parS-4
parS-334
Smc(E1118Q)
amyE
3
4
0
1
2

Figure S6

II.) Supplemental Table

Supplemental Table 1 Genotypes

All strains are derivatives of *Bacillus subtilis* 1A700 provided by the BGSC (*Bacillus* Genetic Stock Center). All strains are auxotrophic for tryptophan (*trpC2*).

BSG1002	smc ftsY::ermB
BSG1007	Δsmc ftsY::ermB
BSG1008	smc(E1118Q) ftsY::ermB
BSG1016	smc-TAP ftsY::ermB
BSG1045	smc(K37I) ftsY::ermB
BSG1046	smc(S1090R) ftsY::ermB
BSG1047	smc(D1117A) ftsY::ermB
BSG1051	smc ftsY::ermB, parAB::kanR
BSG1052	smc ftsY::ermB, ΔparB::kanR
BSG1067	smc-mGFPmut1 ftsY::ermB
BSG1068	smc(E1118Q)-mGFP1mut1 ftsY::ermB
BSG1083	smc(R57A) ftsY::ermB
BSG1360	smc(C119S, C437S, C826S, C1114S)-TEV-His12-HaloTag(C61V, C262A) ftsY::ermB
BSG1378	smc-mGFPmut1 ftsY::ermB, specR::ΔscpA
BSG1387	smc(E1118Q) ftsY::ermB, ΔparB::kanR
BSG1406	smc(E1118Q) ftsY::ermB, parAB::kanR
BSG1413	smc(E1118Q)-mGFP1mut1 ftsY::ermB, specR::ΔscpA
BSG1457	smc(C119S, C437S, C826S, C1114S, K1151C)-TEV-His12-HaloTag(C61V, C262A) ftsY::ermB
BSG1469	smc ftsY::ermB, ΔamyE::parS-359::cat
BSG1470	smc ftsY::ermB, ΔamyE::mtparS-359::cat
BSG1471	smc(E1118Q) ftsY::ermB, ΔamyE::parS-359::cat
BSG1472	smc(E1118Q) ftsY::ermB, ΔamyE::mtparS-359::cat
BSG1475	smc(E1118Q)-TAP ftsY::ermB
BSG1488	smc(C119S, C437S, C826S, C1114S, K1151C, E1118Q)-TEV-His12-HaloTag(C61V, C262A) ftsY::ermB
BSG1509	smc(C119S, C437S, C826S, C1114S, K1151C)-TEV-His12-HaloTag(C61V, C262A) ftsY::ermB, specR::ΔscpA
BSG1512	smc(C119S, C437S, C826S, C1114S, K1151C, E1118Q)-TEV-His12-HaloTag(C61V, C262A) ftsY::ermB, specR::ΔscpA
BSG1513	smc(C119S, C437S, C826S, C1114S, K1151C, E1118Q)-TEV-His12-HaloTag(C61V, C262A) ftsY::ermB, specR::scpA ΔscpB
BSG1520	smc(E1118Q)-TAP ftsY::ermB, specR::ΔscpA
BSG1547	smc(G657A, G658A, G662A, G663A, E1118Q)-ftsY::ermB
BSG1597	smc(C119S, C437S, G657A, G658A, G662A, G663A, C826S, C1114S, K1151C)-TEV-His12-HaloTag(C61V, C262A) ftsY::ermB
BSG1598	smc(C119S, C437S, G657A, G658A, G662A, G663A, C826S, C1114S, E1118Q, K1151C)-TEV-His12-HaloTag(C61V, C262A) ftsY::ermB
BSG1607	smc(K37I, C119S, C437S, C826S, C1114S, K1151C)-TEV-His12-HaloTag(C61V, C262A) ftsY::ermB
BSG1619	rncS smc(1-499 GGGSGGGSGGG 674-1186, E1118Q) ftsY::ermB
BSG1620	smc(G657A, G658A, G662A, G663A, E1118Q)-ftsY::ermB, specR::ΔscpA
BSG1621	smc(G657A, G658A, G662A, G663A, E1118Q)-ftsY::ermB, specR::scpAB
BSG1624	smc(G657A, G658A, G662A, G663A) ftsY::ermB, specR::scpAB
BSG1626	rncS smc(1-499 GGGSGGGSGGG 674-1186) ftsY::ermB
BSG1662	smc(G657A, G658A, G662A, G663A, E1118Q)-mGFP-ftsY::ermB
BSG1671	smc(G657A, G658A, G662A, G663A, E1118Q)-TAP-ftsY::ermB, specR::scpAB
BSG1672	smc(G657A, G658A, G662A, G663A)-TAP ftsY::ermB, specR::ΔscpA
BSG1677	smc(G657A, G658A, G662A, G663A)-mGFP-ftsY::ermB

BSG1689	smc(G657A, G658A, G662A, G663A, E1118Q)-TAP ftsY::ermB, specR::ΔscpA
BSG1691	smc(G657A, G658A, G662A, G663A)-TAP ftsY::ermB, specR::scpAB
BSG1779	smc(1-499 GGGSGGGSGGG 674-1186, E1118Q)-TAP::ermB, specR::ΔscpA
BSG1780	smc(1-499 GGGSGGGSGGG 674-1186, E1118Q)-TAP::ermB, specR::scpAB
BSG1791	smc(C119S, C437S, G657A, G658A, G662A, G663A, C826S, C1114S, E1118Q, K1151C)-TEV-His12-HaloTag(C61V, C262A) ftsY::ermB, specR::ΔscpA
BSG1798	smc(G657A, G658A, G662A, G663A, E1118Q)-mGFP-ftsY::ermB, specR::ΔscpA
BSG1799	smc(G657A, G658A, G662A, G663A)-mGFP-ftsY::ermB, specR::ΔscpA
BSG1800	smc(C119S, C437S, G657A, G658A, G662A, G663A, C826S, C1114S, K1151C)-TEV-His12-HaloTag(C61V, C262A) ftsY::ermB, specR::ΔscpA
BSG1824	smc(1-199 GGGSGGGSGGG 999-1186, E1118Q)-TAP::ermB, specR::ΔscpA
BSG1825	smc(1-219 GPG 983-1186, E1118Q)-TAP::ermB, specR::ΔscpA
BSG1826	smc(1-243 GGGSGGGSGGG 957-1186, E1118Q)-TAP::ermB, specR::ΔscpA
BSG1827	smc(1-243 GGGSGGGSGGG 943-1186, E1118Q)-TAP::ermB, specR::ΔscpA
BSG1828	smc(1-261 GGGSGGGSGGG 943-1186, E1118Q)-TAP::ermB, specR::ΔscpA
BSG1829	smc(1-261 GGGSGGGSGGG 912-1186, E1118Q)-TAP::ermB, specR::ΔscpA
BSG1830	smc(1-277 GGGSGGGSGGG 922-1186, E1118Q)-TAP::ermB, specR::ΔscpA
BSG1855	smc(K37I)-mGFP1mut1 ftsY::ermB
BSG1856	smc(S1090R)-mGFP1mut1 ftsY::ermB
BSG1857	smc(D1117A)-mGFP1mut1 ftsY::ermB
BSG1871	smc(1-468 GGGSGGGSGGG 705-1186, E1118Q)-TAP::ermB, specR::ΔscpA
BSG1872	smc(1-437 GGGSGGGSGGG 736-1186, E1118Q)-TAP::ermB, specR::ΔscpA
BSG1873	smc(1-315 GGGSGGGSGGG 858-1186, E1118Q)-TAP::ermB, specR::ΔscpA
BSG1874	smc(1-370 GGGSGGGSGGG 803-1186, E1118Q)-TAP::ermB, specR::ΔscpA
BSG1875	smc(1-414 GGGSGGGSGGG 785-1186, E1118Q)-TAP::ermB, specR::ΔscpA
BSG1881	smc(R57A)-mGFP1mut1 ftsY::ermB
BSG1889	smc ftsY::ermB, specR::ΔscpA
BSG1890	smc ftsY::ermB, specR::scpAB
BSG1891	smc ftsY::ermB, specR::scpA ΔscpB
BSG1892	smc(E1118Q) ftsY::ermB, specR::ΔscpA
BSG1893	smc(E1118Q) ftsY::ermB, specR::scpAB
BSG1895	smc(1-499 GGGSGGGSGGG 674-1186)-TAP ftsY::ermB, specR::ΔscpA
BSG1896	smc(1-499 GGGSGGGSGGG 674-1186)-TAP ftsY::ermB, specR::scpAB
BSG1921	smc(C119S, C437S, A715C, C826S, C1114S)-TEV-His12-HaloTag(C61V, C262A) ftsY::ermB
BSG1922	smc(C119S, C437S, A715C, C826S, C1114S, E1118Q)-TEV-His12-HaloTag(C61V, C262A) ftsY::ermB
BSG1923	smc(C119S, C437S, G657A, G658A, G662A, G663A, A715C, C826S, C1114S)-TEV-His12-HaloTag(C61V, C262A) ftsY::ermB
BSG1924	smc(C119S, C437S, G657A, G658A, G662A, G663A, A715C, C826S, C1114S, E1118Q)-TEV-His12-HaloTag(C61V, C262A) ftsY::ermB
BSG1949	smc(C119S, C437S, A715C, C826S, C1114S)-TEV-His12-HaloTag(C61V, C262A) ftsY::ermB, specR::ΔscpA
BSG1950	smc(C119S, C437S, A715C, C826S, C1114S, E1118Q)-TEV-His12-HaloTag(C61V, C262A) ftsY::ermB, specR::ΔscpA
BSG1951	smc(C119S, C437S, G657A, G658A, G662A, G663A, A715C, C826S, C1114S)-TEV-His12-HaloTag(C61V, C262A) ftsY::ermB, specR::ΔscpA
BSG2036	smc(C119S, C437S, G657A, G658A, G662A, G663A, A715C, C826S, C1114S, E1118Q)-TEV-His12-HaloTag(C61V, C262A) ftsY::ermB, specR::ΔscpA
BSG2050	smc(K37I, E1118Q) ftsY::ermB
BSG2051	smc(S1090R, E1118Q) ftsY::ermB
BSG2144	specR::scpAB, smc(G657A, G658A, G662A, G663A, E1118Q)-ftsY::ermB
BSG2145	specR::ΔscpA, smc(G657A, G658A, G662A, G663A, E1118Q)-ftsY::ermB
BSG2146	specR::scpA ΔscpB, smc(G657A, G658A, G662A, G663A, E1118Q)-ftsY::ermB
BSG2147	specR::ΔscpAB, smc(G657A, G658A, G662A, G663A, E1118Q)-ftsY::ermB

III.) Supplemental Experimental Procedures

In vivo expression of Smc proteins tested by immunoblotting

Cells were grown in SMG at 37°C to an OD_{600} of 0.02-0.03, harvested by centrifugation or filtrations and washed once in 2 ml PBSG (PBS + 0.1% glycerol). The OD_{600} was measured and equivalent amount of cells for all samples were taken (0.02 ml*OD_{600}). Cells were resuspended in PBSG, ß-mercaptoethanol was added to a final concentration of 28.6 mM and kept on ice for 3 min. Lysozyme (12.8U/µl final), *Roche Complete* protease inhibitor cocktail and Benzonase (0.4 U/µl; Sigma-Aldrich) were added and the samples were incubated at 37°C for 20 min. NuPage LDS loading dye (final 1x) and DTT (final conc. 100 mM) were added and the samples incubated at 70°C for 10 min. The extracts were loaded on a 4-12% NuPAGE Bis-Tris gel run in MOPS buffer for 50 min at 200 V. Proteins were transferred to a PVDF membrane which was treated with α-Smc, α-GFP (Life Technologies, A6455) or Peroxidase Anti-Peroxidase (PAP). α-Smc and α-GFP blots were treated with ECL Anti-rabbit IgG, HRP-linked whole antibody (from donkey) (GE healthcare). The blots were incubated with Supersignal West Femto (Thermo Scientific) and were imaged in a LAS4000 scanner.

Chromatin immuno-precipitation (ChIP) and qPCR

Cells were grown in SMG medium at 37ºC overnight and diluted to OD_{600} 0.005 in SMG. At OD 0.02-0.03 40 ml of fixing solution (50mM Tris/HCl pH 8.0, 100mM NaCl, 1mM EDTA, 0.5mM EGTA, 11% formaldehyde) was added to 400 ml of culture and incubated at room temperature for 30 minutes. Cells were harvested by centrifugation or filtration and washed in 2 ml ice-cold PBS and OD_{600} was measured. Cells were resuspended in 1 ml TESS (50mM Tris/HCl 7.4, 10mM EDTA, 50mM NaCl, 500mM sucrose) and protoplasted by incubating in 1 ml TESS supplemented with 20mg/ml lysozyme (Sigma) and Roche Complete protease inhibitor cocktail for 30 min at 37°C shaking. Cells were washed once in 1 ml TESS, aliquoted according to the previously measured OD_{600} and stored at -80°C.

One aliquot of fixed cells was resuspended in 2 ml lysis buffer (50mM Hepes/KOH pH 7.5, 140mM NaCl, 1mM EDTA, 1% (v/v) Triton X-100, 0.1% (w/v) sodium deoxycholate, 100mg/ml RNase, *Roche Complete* protease inhibitor cocktail) and transferred to a 5 ml round-bottom tube. The samples were sonicated 3 x 20 sec on a Bandelin Sonoplus with a MS-72 tip at 90% pulse and 35% power output. Lysates were transferred into 2 ml tubes and centrifuged 5 min at 21000g and the supernatant subsequently 10 min at 21000g at 4°C.

200 µl of the cleared lysates was kept separate as the input sample. 50 µl Protein G coupled dynabead (Invitrogen) were incubated with 50 µl antibody serum (α-Smc, α-ScpB or α-ParB generated in rabbit) for at least 1 hr rotating at 4°C. Beads were washed in lysis buffer and added to 800 µl of the cleared lysates. For experiments involving TAP-tagged strains, rabbit IgG coupled to 50 µl magnetic DynaBeads (Epoxy, M-270) (prepared according to the manufacturer's protocol) was added to 800 µl cleared lysates. The beads with cleared lysates were incubated at 4°C rotating for 2-4 hours. Beads were washed once with each of the following buffers, lysis buffer, lysis buffer with high salt (500mM NaCl) and wash buffer (10mM Tris/HCl pH 8.0, 250mM LiCl, 1mM EDTA, 0.5% (w/v) NP-40, 0.5% (w/v) sodium deoxycholate). Beads were resuspended in 520 µl TES (50mM Tris/HCl pH 8.0, 10mM EDTA, 1% SDS), the input samples were combined with 300 µl TES and 20 µl 10% SDS solution and incubated overnight at 65°C shaking. DNA was purified by phenol chloroform extraction and ethanol precipitation. The DNA was dissolved in 100µl TE at 65°C for 20 min and purified on a Qiagen PCR purification column and eluted in 30 µl EB. For qPCR 4 µl of the input DNA (diluted 1:200) and IP samples (diluted 1:20) was used in a 10 µl reaction using 5 µl Takyon no ROX SYBR Mastermix blue dTTP (Eurogentec) and 1 µl primer pair stock solution (3 µM each primer) on a Qiagen Rotor-Gene Q in a 72 well rotor according to manufacturer's instructions. Primer sequences are given in the table below. Curves were analyzed by determining the maximum of the 2nd derivative using the Real-time PCR miner software (http://ewindup.info) (Zhao and Fernald, 2005). ChIP efficiencies were calculated as follows: [(IP/input)*100] for each primer pair.

List of primer pairs for qPCR:

parS-356	STG236	tgaaaagaatgcccatcaca
	STG237	tgcaagcaacaaccctttac
parS-359	STG097	aaaaagtgattgcggagcag
	STG098	agaaccgcatctttcacagg
dnaA	STG199	gatcaatcggggaaagtgtg
	STG200	gtagggcctgtggatttgtg
trnS	STG404	gggttttgacaccttggta
	STG405	aagcaaaaggaaatggctga
cheC	STG396	tttgcatgaactgggcaata
	STG397	tccgaacatgtccaatgaga
yocGH	STG099	tccatatcctcgctcctacg
	STG100	attctgctgatgtgcaatgg

Protein purification and SEC-MALS

Wild-type and hinge mutant *Bs*SmcH-CC300 protein (Smc residues 188-1011) were overexpressed from plasmid pnEA-tH in *E. coli* with an N-terminal HISx6 tag (Diebold et al., 2011). The proteins were purified via a HisTrap column, concentrated by anion-exchange chromatography (MonoQ HiTrap) and eluted from a size exclusion chromatography column (Superdex 200 10/300) in 200mM NaCl, 25mM Tris/HCl pH 7.4 (4°C). Multi-angle light scattering coupled to size exclusion chromatography (SEC-MALS) was performed as described previously (Soh et al., 2015).

Viability spotting assay

Cells were grown in SMG medium overnight into stationary phase, diluted 81-fold and 59049-fold (in 9x steps) and spotted on nutrient agar plates (Oxoid) or SMG agar plates. Plates were incubated at 37°C for ~12 hr on NA or ~36 hr on SMG agar.

Mapping of the *Bs* Smc coiled coil register by disulfide formation

Intramolecular crosslinking reactions for the determination of the coiled coil register were performed essentially as described in (Waldman et al., 2015) using the BsSmcH-CC300 construct (Soh et al., 2015). The protein was expressed from the pnEA-tH plasmid as a His-Tag fusion protein. For each double cysteine mutant, 50mL cultures were set-up. Cells were lysed by sonication and soluble extract was incubated for one hour with 300uL of Talon resin (Clontech). Beads were washed three times with the lysis buffer (200 mM NaCl, 50 mM NaPi pH7.4, 5 mM Imidazole) and then resuspended in the lysis buffer supplemented with 1 mM magnesium chloride. 1uL of benzonase (Roche) was added to the beads that were shaked for 30min at room temperature to remove the bound DNAs. The beads were washed two more times with the lysis buffer and the proteins were eluted with elution buffer 200 mM NaCl, 500 mM Imidazole, 50 mM NaPi pH7.4.

The proteins were then dialyzed against PBS buffer containing 4 mM DTT for 2 hours. For the crosslinking reaction, the protein was diluted to a concentration of 5 µM. The non-crosslinked sample was prepared by adding 1mM of iodoacetamide and heating at 70°C for 10 min. Disulfide formation was set-up by adding one volume of PBS supplemented with 5 mM $NaAsO_2$ (Fluka) to the protein and 100 µM dithio-bisnitrobenzoic acid DTNB (Merck) and 300 µM beta-mercaptoethanol. The reaction was incubated at 4°C under shaking. Samples were taken after 2, 4, 6 and 20h of reaction, and quenched by addition of 10 mM iodoacetamide at 70°C for 10 min.

After addition of non-reducing SDS-Page loading buffer the samples were boiled for 5 min at 95°C and run on a Bis-Tris 4-16% NuPage acrylamide gel (Novex) using MOPS buffer as running buffer for 50 min at 200 V.

IV.) Supplemental References

Diebold, M.L., Fribourg, S., Koch, M., Metzger, T., and Romier, C. (2011). Deciphering correct strategies for multiprotein complex assembly by co-expression: application to complexes as large as the histone octamer. Journal of structural biology *175*, 178-188.

Gruber, S., and Errington, J. (2009). Recruitment of condensin to replication origin regions by ParB/SpoOJ promotes chromosome segregation in B. subtilis. Cell *137*, 685-696.
Gruber, S., Haering, C.H., and Nasmyth, K. (2003). Chromosomal cohesin forms a ring. Cell *112*, 765-777.

Kleine Borgmann, L.A., Ries, J., Ewers, H., Ulbrich, M.H., and Graumann, P.L. (2013). The bacterial SMC complex displays two distinct modes of interaction with the chromosome. Cell reports *3*, 1483-1492.

Schwartz, M.A., and Shapiro, L. (2011). An SMC ATPase mutant disrupts chromosome segregation in Caulobacter. Molecular microbiology *82*, 1359-1374.

Soh, Y.M., Burmann, F., Shin, H.C., Oda, T., Jin, K.S., Toseland, C.P., Kim, C., Lee, H., Kim, S.J., Kong, M.S., *et al.* (2015). Molecular basis for SMC rod formation and its dissolution upon DNA binding. Molecular cell *57*, 290-303.

Waldman, V.M., Stanage, T.H., Mims, A., Norden, I.S., and Oakley, M.G. (2015). Structural mapping of the coiled-coil domain of a bacterial condensin and comparative analyses across all domains of life suggest conserved features of SMC proteins. Proteins *83*, 1027-1045.

Wang, X., Tang, O.W., Riley, E.P., and Rudner, D.Z. (2014). The SMC condensin complex is required for origin segregation in Bacillus subtilis. Current biology : CB *24*, 287-292.